Mathematics

https://www.aimspress.com/journal/Math

AIMS Mathematics, 11(8): 27203–27230.
DOI: 10.3934/math.20261089
Received: 26 June 2026
Revised: 12 August 2026
Accepted: 19 August 2026
Published: 28 August 2026

Research article

Intermittent event-triggered impulsive control for consensus of delayed multi-agent systems subject to deception attacks

Chen Liu[1,2,*], **Mengting Wang**[1], **Qing Chen**[1] **and Yihao Chu**[1]

[1] School of Mathematics and Statistics, Anqing Normal University, Anqing, 246133, China
[2] Key Laboratory of Modeling, Simulation and Control of Complex Ecosystem in Dabie Mountains of Anhui Higher Education Institutes, Anqing, 246133, China

* **Correspondence:** Email: liuchen_hhu@163.com.

Abstract: This paper focus on the mean-square quasiconsensus issue in delayed leader-following multi-agent systems. An event-triggered intermittent impulsive control is developed to ensure consensus for systems facing deception attacks. First, a closed-loop intermittent control scheme is developed. In this framework, the working intervals are determined by a Lyapunov-based event-triggered mechanism (ETM), which adjusts the control activation according to real-time system states. Furthermore, a newly proposed delayed differential inequality featuring piecewise characteristics is constructed to address these analytical challenges arising from the integration of state-based intermittent control, state delay, deception attacks, and impulsive control. The proposed inequality further leads to a sufficient criterion under which the considered systems achieve mean-square quasiconsensus. Simulation results are reported to show that the proposed conditions are applicable.

Keywords: delayed multi-agent systems; consensus; deception attacks; event-triggered mechanism; impulsive control
Mathematics Subject Classification: 93C10, 93D15

1. Introduction

A multi-agent system (MAS) consists of several autonomous units linked by local information exchange. These units can perceive environmental changes, process information, and perform actions independently. Cooperative control of MASs focus on developing distributed control strategies that allow agents to collaborate within dynamic environments to achieve global objectives such as consensus [1], formation [2], and clustering [3]. Such methodologies have been extensively deployed in various engineering scenarios, such as distributed sensor arrays [4], multi unmanned aerial vehicle (UAV) cooperative flights [5], and smart grids [6]. Leader-following consensus is a fundamental issue in distributed coordination, which aims to drive followers toward the leader state and provides a theoretical foundation for formation and tracking problems. Recently, Xu et al. [7] studied the prescribed-performance bipartite consensus for linear MASs via a time-varying barrier Lyapunov function-based gain method. However, MASs are inevitably subject to communication and processing delays. Therefore, the study of the consensus problem in MASs with delays is of great theoretical significance.

Intermittent control is characterized by its discontinuous actuation and serves as an effective strategy for systems subject to intermittent communication. It offers high flexibility, with classifications based on communication cycles (periodic/aperiodic). Yu et al. [8] studied second-order consensus in MASs via periodic intermittent control. Later, He et al. [9] successfully resolved the finite-time consensus issue for linear MASs through the application of aperiodic intermittent control. For delayed MASs, the study in [10] explored state-tracking protocols for nonlinear MASs utilizing an aperiodic intermittent communication mechanism. By employing an innovative aperiodic intermittent control scheme, exponential consensus for delayed MASs was successfully analyzed in [11]. Xiao et al. [12] explored the bipartite agreement task for MASs with delays through the application of an aperiodic intermittent control scheme. It is important to note that current advances in intermittent control predominantly rely on open-loop strategies with fixed timing sequences. Consequently, the design of a closed-loop framework capable of real-time adaptation to system states remains a critical and unresolved challenge. This work is motivated by the critical need to overcome the limitations of static open-loop schemes through real-time adaptive control.

A significant benefit of the event-triggered mechanism (ETM) is its ability to substantially decrease the number of control task executions by dynamically scheduling triggering instants based on real-time system state monitoring [13]. In 2009, Dimarogonas et al. [14] pioneered the introduction of ETMs into the research of MASs, providing a new perspective for solving consensus problems in MASs. Xie et al. [15] considered a distributed ETM applicable to nonlinear MASs with dynamics of either first or second order. Zhao et al. [16] guaranteed leader-following synchronization for MASs possessing second-order dynamics through an event-based approach. Zhang et al. [17] proposed an adaptive temporal partitioning strategy for communication-efficient consensus in nonlinear MASs. Pan et al. [18] developed an event-triggered predefined-time control strategy for full-state constrained nonlinear systems by introducing a novel command-filtering error compensation method. Leveraging the complementary advantages of intermittent control and ETMs, their integration has garnered increasing research attention for addressing consensus problems in MASs. Hu et al. [19] investigated intermittent dynamic ETM in the case of consensus control for MASs. For nonlinear MASs, Liang et al. [20] studied consensus tracking under a hybrid strategy that integrates event-triggered updates and intermittent control. Liu et al. [21] established an intermittent event-based mechanism for realizing optimal leader-following consensus in MASs experiencing communication delays. However, current intermittent event-triggered strategies often rely on a mechanical superposition of control policies, where the control intervals are predetermined and lack real-time interaction with system states, limiting their adaptability in complex dynamic environments. Consequently, research is shifting toward closed-loop integration, with a key breakthrough being the dynamic determination of control intervals' start and end points via ETM, thereby achieving deep coupling between control actions and system states. For nonlinearly coupled complex networks, Zhu et al. [22] developed an aperiodic intermittent pinning control method to ensure exponential cluster synchronization. Liu et al. [23] focused on stabilizing delayed dynamical systems by utilizing an intermittent regulation with a dynamic ETM. Ma et al. [24] studied the consensus for delayed MASs possessing nonlinear characteristics by proposing a novel distributed intermittent control with an ETM.

Impulsive control is a control strategy that performs instantaneous adjustments to system states at discrete instants, featuring prominent advantages such as fast response speed and low energy consumption, and serves as an efficient approach to tackle the consensus problem in MASs. Ma et al. [25] examined consensus in MASs with nonlinear dynamics satisfying a one-sided Lipschitz condition under impulsive effects and semi-Markovian switching topologies. Tang et al. [26] developed a consensus scheme based on event-triggered impulses for uncertain MASs evolving over directed communication topologies. To achieve bipartite consensus within a finite time horizon for nonlinear MASs, an event-based intermittent impulsive framework was developed by Wang et al. [27]. For nonlinear delayed MASs with hybrid delays, the leader-following consensus issue was studied in [28] through distributed impulsive control. Wang et al. [29] addressed average consensus in delayed nonlinear MASs using an impulsive control method based on ETM. Zhang et al. [30] studied synchronization in delayed complex networks by combining event-triggering, intermittent actuation, and impulsive intervention within a unified control framework.

Deception attacks, as a typical type of cyber attack, mislead system control decisions by forging transmitted information and tampering with interactive data, posing a significant threat to the safe and stable operation of MASs [31]. Deception attacks may degrade the control performance and even destabilize networked control systems. Zong et al. [32] developed an adaptive fuzzy tracking controller for switched nonlinear systems subject to false data injection (FDI) attacks and input saturation. For MASs subject to deception attacks, secure control and synchronization have been extensively investigated in [33–36]. In particular, Yin et al. [33] developed an event-based intermittent formation control approach for multi-UAV systems encountering deception attacks. Different from these works, Liu et al. [34] studied the secure consensus of attacked MASs from an impulsive control perspective. Zhao et al. [35] combined impulsive control with an ETM to preserve consensus security when deception attacks occur. For stochastic neural networks, Zhou et al. [36] investigated secure synchronization and employed an event-driven intermittent impulsive controller to cope with such attacks.

Despite substantial progress in intermittent, event-triggered, and impulsive control, several issues remain to be further addressed. Zhang et al. [30] and Wang et al. [37] considered delayed systems under event-triggered intermittent impulsive control and aperiodic intermittent control, respectively, whereas deception attacks were not considered. Liu et al. [34] and Zhou et al. [36] addressed secure control under deception attacks through impulsive or event-based intermittent impulsive control, but state delays were not simultaneously incorporated. Moreover, none of these studies simultaneously considered state delays, deception attacks, dynamically generated working-resting intervals, a forced check-period, or impulsive control within a unified framework. This paper addresses the quasiconsensus of MASs with state delays affected by deception attacks by using intermittent control and an ETM. The main results are listed as follows:

(1) Different from the control schemes in [30] and [34], the proposed Lyapunov-based ETM dynamically determines the working intervals according to the real-time system state and incorporates a forced check-period to prevent excessively long silence intervals between successive control updates.

(2) Different from [30,34,36,37], which consider only partial combinations of state delay, deception attacks, event-triggered intermittent control, and impulsive effects, a new, delay-dependent piecewise differential inequality is established to characterize the strongly coupled evolution of these factors within a unified Lyapunov framework (see Table 1). In particular, it explicitly relates the event-triggered sequence, dynamically generated working-resting intervals, and attack-affected impulsive jumps, thereby enabling the derivation of sufficient conditions and an explicit ultimate error bound for leader-following mean-square quasiconsensus.

(3) By employing Lyapunov analysis, a sufficient condition is derived under which the delayed leader-following MASs can achieve mean-square quasiconsensus despite deception attacks.

Table 1. Comparison between former publications and this work.

Feature	[30]	[34]	[36]	[37]	This paper
State delay	✓	×	×	✓	✓
Deception attack	×	✓	✓	×	✓
Event triggering	✓	×	✓	✓	✓
Forced check-period	✓	×	✓	✓	✓
Dynamic intermittent intervals	×	×	✓	✓	✓
Impulsive control	✓	✓	✓	×	✓

✓: Considered; ×: Not considered.

2. Preliminaries and system modeling

2.1. Graph theory

The communication relationship among agents is modeled by a directed graph $\mathbb{G} = (\mathbb{V}, \widetilde{\mathbb{E}})$. The node set contains one leader and N followers, where the leader is labeled by 0, and the followers are indexed by $\mathcal{I} = \{1, 2, \ldots, N\}$. An edge $(j, i) \in \widetilde{\mathbb{E}}$ means that agent i is able to access the information of agent j. For each follower i, its neighbor set is written as $\mathcal{N}_i = \{j \in \mathcal{I} : (j, i) \in \widetilde{\mathbb{E}}\}$. The weighted adjacency matrix among followers is denoted by $\mathcal{A} = [a_{ij}] \in \mathbb{R}^{N\times N}$, where $a_{ij} > 0$ if $(j, i) \in \widetilde{\mathbb{E}}$ and $a_{ij} = 0$ otherwise. Define $\mathcal{D} = \mathrm{diag}(d_1, \ldots, d_N)$ with $d_i = \sum_{j\in\mathcal{N}_i} a_{ij}$. Then, the Laplacian matrix is given by $\mathbb{L} = \mathcal{D} - \mathcal{A}$. The connection between the leader and the followers is described by $\mathbb{B} = \mathrm{diag}(\beta_1, \ldots, \beta_N)$, where $\beta_i > 0$ when follower i can directly receive the leader's information, and $\beta_i = 0$ otherwise. Thus, the leader-following topology matrix is written as $\mathcal{H} = \mathbb{L} + \mathbb{B}$.

The next assumption and lemma describe the connectivity requirement used in the subsequent analysis.

Assumption 2.1. *[38] In the directed graph $\mathbb{G}$, the leader has a directed path to every follower, so that the reference information generated by the leader can be transmitted to all followers.*

Lemma 2.1. *[39] Let $\mathcal{H}$ be a nonsingular M-matrix. Then, there exists a diagonal matrix $P > 0$ such that $P\mathcal{H} + \mathcal{H}^\top P > 0$.*

2.2. Mathematical lemmas

This subsection gives several auxiliary results for the subsequent analysis. They help estimate delayed-state terms, bound the consensus error, and derive mean-square quasiconsensus criteria for the closed-loop system.

Lemma 2.2. *[40] Introduce $\varrho(t)$ as a function taking non-negative values over the interval $[-\varsigma, +\infty)$. If*

$$\dot{\varrho}(t) \leq -c_1\varrho(t) + c_2\varrho(t-\varsigma), \quad t \geq 0,$$

where $c_1 > c_2 > 0$, then $\varrho(t) \leq \tilde{\varrho}(0)e^{-rt}$, where $\tilde{\varrho}(0) = \sup_{-\varsigma\leq s\leq 0}\varrho(s)$, and $r > 0$ satisfies

$$-r = -c_1 + c_2 e^{r\varsigma}.$$

Lemma 2.3. *[41] Introduce $\varrho(t)$ as a function taking non-negative values over the interval $[-\varsigma, +\infty)$. If*

$$\dot{\varrho}(t) \leq c_1\varrho(t) + c_2\varrho(t-\varsigma), \quad t \geq 0,$$

with $c_1 > 0$ and $c_2 > 0$, then $\varrho(t) \leq \tilde{\varrho}(0)e^{(c_1+c_2)t}$.

Lemma 2.4. *[39] Let u and v be arbitrary vectors in $\mathbb{R}^m$, and let $\mathcal{S} \in \mathbb{R}^{m\times m}$ be a symmetric positive definite matrix. Then, $u^\top v + v^\top u \leq \epsilon u^\top \mathcal{S} u + \epsilon^{-1} v^\top \mathcal{S}^{-1} v$ for every $\epsilon > 0$.*

2.3. System formulation

For a delayed MAS with exactly one leader and N followers, its mathematical description is given by

$$\begin{cases} \dot{\mathcal{X}}_0(t) = \mathfrak{R}\left(t, \mathcal{X}_0(t), \mathcal{X}_0(t-\varsigma)\right), \\ \dot{\mathcal{X}}_i(t) = \mathfrak{R}\left(t, \mathcal{X}_i(t), \mathcal{X}_i(t-\varsigma)\right) + u_i(t), \quad i = 1, 2, \cdots, N, \end{cases} \tag{2.1}$$

where $\mathcal{X}_0(t) \in \mathbb{R}^n$ and $\mathcal{X}_i(t) \in \mathbb{R}^n$ correspond to the leader and follower states, respectively. $\mathfrak{R}$ represents the nonlinear part in the dynamics of each agent, and $u_i(t)$ is the control input assigned to follower i. Define the state error by $\xi_i(t) = \mathcal{X}_i(t) - \mathcal{X}_0(t)$. Thus, the error dynamics of (2.1) are given by

$$\dot{\xi}_i(t) = \tilde{\mathfrak{R}}(t, \xi_i(t), \xi_i(t-\varsigma)) + u_i(t), \tag{2.2}$$

where $\tilde{\mathfrak{R}}(t, \xi_i(t), \xi_i(t-\varsigma)) = \mathfrak{R}(t, \mathcal{X}_i(t), \mathcal{X}_i(t-\varsigma)) - \mathfrak{R}(t, \mathcal{X}_0(t), \mathcal{X}_0(t-\varsigma))$.

Assumption 2.2. *[35] The mapping $\mathfrak{R}(t,\cdot,\cdot)$ is Lipschitz continuous; that is, there exist constants $\gamma_1, \gamma_2 > 0$ such that for all $\hbar_1, \hbar_2, \hat{\hbar}_1, \hat{\hbar}_2 \in \mathbb{R}^n$,*

$$\|\mathfrak{R}(t, \hbar_1, \hbar_2) - \mathfrak{R}(t, \hat{\hbar}_1, \hat{\hbar}_2)\| \leq \gamma_1\|\hbar_1 - \hat{\hbar}_1\| + \gamma_2\|\hbar_2 - \hat{\hbar}_2\|. \tag{2.3}$$

Definition 2.1. *[42] Given arbitrary initial states $\xi_i(0)$ for all agents, the targeted leader-following mean-square quasiconsensus is realized when there emerges a positive ultimate error bound $\mathcal{B} > 0$ such that*

$$\limsup_{t\to\infty} \mathbb{E}\{V(\xi(t))\} \leq \mathcal{B}.$$

3. Proposed event-based intermittent impulsive control

This section systematically formulates the essential regulatory framework to guarantee the quasi-consensus of the MAS. To effectively counteract deception attacks while simultaneously alleviating the communication burden, the proposed hybrid framework is developed step by step.

3.1. Closed-loop intermittent control

To save energy, an intermittent control strategy is adopted for system (2.2), formulated as

$$\begin{cases} \dot{\xi}_i(t) = \tilde{\mathfrak{R}}(t, \xi_i(t), \xi_i(t-\varsigma)) + u_i(t), & t \in [t_k, s_k), \\ \dot{\xi}_i(t) = \tilde{\mathfrak{R}}(t, \xi_i(t), \xi_i(t-\varsigma)), & t \in [s_k, t_{k+1}). \end{cases} \tag{3.1}$$

Let $w_k = s_k - t_k > 0$ denote the prescribed duration of the kth working interval. Accordingly, the ending instant of the working interval is given by $s_k = t_k + w_k$. The controller is active on $[t_k, s_k)$ and is switched off at s_k. Figure 1 depicts the control timeline; the system timeline is divided into a working window $[t_k, s_k)$ triggered by the ETM at t_k, and a dormant window $[s_k, t_{k+1})$ that commences at s_k once the controller is disabled.

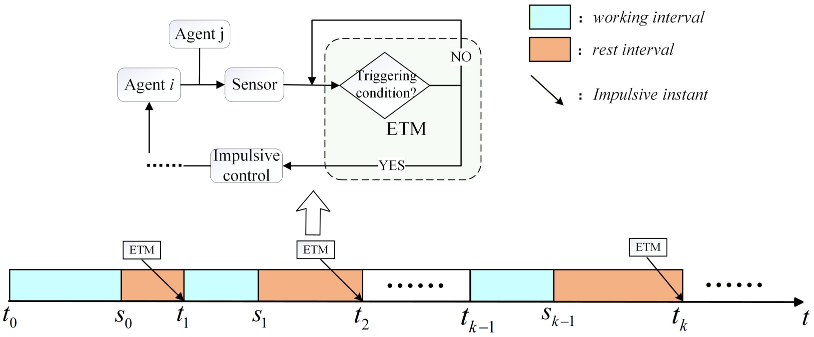

Figure 1. Schematic of the closed-loop intermittent control.

A Lyapunov-type event-triggering rule is adopted in the intermittent control process to avoid unnecessary updates. Let η be the triggering coefficient. Then, t_{k+1} is determined by

$$t_{k+1} = \inf\left\{ t > s_k : \ V(\xi(t)) > e^{\eta} V(\xi(t_k)) \right\}. \tag{3.2}$$

However, traditional control strategies often suffer from the "silence" problem. To overcome this limitation, this paper designs an ETM with a check-period Λ, formulated as

$$\begin{cases} t^*_{k+1} = \inf\left\{ t > s_k : \ V(\xi(t)) > e^{\eta} V(\xi(t_k)) \right\}, \\ t_{k+1} = \min\left\{ t^*_{k+1}, \ t_k + \Lambda \right\}. \end{cases} \tag{3.3}$$

Remark 3.1. *A limitation of the conventional ETM* (3.2) *is that t_{k+1} would never be updated whenever $V(\xi(t)) \leq e^{\eta} V(\xi(t_k))$, thereby severely compromising overall robustness. Consequently, to ensure that the closed-loop system operates effectively, an updated triggering condition $t_{k+1} = \min\{t^*_{k+1}, t_k + \Lambda\}$ is employed. For the kth intermittent-control interval, the working interval is $[t_k, s_k)$ with $s_k = t_k + w_k$, where $w_k > 0$, and the resting interval is $[s_k, t_{k+1})$. If the triggering condition is satisfied before $t_k + \Lambda$, then $t_{k+1} = t^*_{k+1}$; otherwise, $t_{k+1} = t_k + \Lambda$. Thus, w_k determines the controller-active duration, and Λ prevents excessively long silence intervals.*

3.2. Impulsive control in the presence of cyber deception

To formulate how the impulsive mechanisms are compromised by deceptive signals, we begin by introducing the attack profile and its associated stochastic properties. Considering that the attackers are energy-limited, let $q_i(t)$ represent the false data injected into agent i. By aggregating these individual signals, the global attack vector is constructed as follows: $Q(t) = \mathrm{col}(q_1(t), q_2(t), \ldots, q_N(t))$. Furthermore, it is hypothesized that this composite attack signal is energy-bounded, satisfying $\|Q(t)\|^2 \leq q$, with the known positive scalar q representing the allowable maximum attack energy. In the considered attack model, the deception attack affects the information used at each impulsive triggering instant t_k, regardless of whether the triggering instant is generated by the state-dependent triggering condition or by the forced checking rule. Therefore, the deception-induced impulsive signal is injected only at the discrete triggering instants rather than continuously during the working or resting intervals.

To counteract deception attack interference on information transmission, we develop a distributed impulsive controller for MASs (2.1):

$$u_i(t) = \sum_{k=1}^{\infty} \delta(t - t_k)\bigg\{ - c\bigg[\sum_{j \in \mathcal{N}_i} \Big(a_{ij}(\mathcal{X}_i(t) - \mathcal{X}_j(t)) - \kappa_{ij}(t) q_i(t) \Big) + \beta_i(\mathcal{X}_i(t) - \mathcal{X}_0(t)) \bigg]\bigg\}, \tag{3.4}$$

where the above control law works for $t \in [t_k, s_k)$, $\delta(t - t_k)$ corresponding to the Dirac delta function centered at t_k, c is the coupling strength. The impulsive sequence $\{t_k\}_{k=0}^{\infty}$ is strictly increasing with $t_0 = 0$ and satisfies $\lim\limits_{k\to\infty} t_k = \infty$. The random variable $\kappa_{ij}(t)$ is assumed to follow a Bernoulli distribution with the probability mass function

$$\mathbb{P}(\kappa_{ij}(t) = m) = \omega_{ij}^m (1 - \omega_{ij})^{1-m}, \qquad m \in \{0, 1\}, \tag{3.5}$$

where $\omega_{ij} \in [0, 1)$ denotes the success probability of the deception attack on link (j, i). Let $\Omega(t_k) = [\kappa_{ij}(t_k)]_{N\times N}$. Then,

$$\mathbb{E}[\Omega(t_k)] = \begin{bmatrix} 0 & \omega_{12} & \cdots & \omega_{1N} \\ \omega_{21} & 0 & \cdots & \vdots \\ \vdots & \vdots & \ddots & \vdots \\ \omega_{N1} & \omega_{N2} & \cdots & 0 \end{bmatrix} = \Gamma.$$

To characterize the timing properties of the intermittent-control sequence, the following average-type assumptions are introduced. These conditions restrict the number of intermittent-control intervals and the accumulated duration of the resting intervals over a given time interval.

Assumption 3.1. *[43] There exist constants $\rho \geq 0$ and $U_D > 0$ such that for any $k > n \geq 0$,*

$$k - n \leq \rho + \frac{t_k - t_n}{U_D}, \tag{3.6}$$

where $k-n$ denotes the number of intermittent-control intervals or equivalently the number of impulsive update instants over $[t_n, t_k)$.

Assumption 3.2. *[43] There exist constants $\varkappa \geq 0$ and $T \geq 1$ such that for any $k > n \geq 0$,*

$$\sum_{i=n+1}^{k} (t_i^- - s_{i-1}) \leq \varkappa + \frac{t_k - t_n}{T}, \tag{3.7}$$

where the summation on the left-hand side denotes the accumulated duration of the resting intervals over $[t_n, t_k)$.

Combining the intermittent ETM and the impulsive controller subject to deception attacks, the resulting closed-loop error system corresponding to (2.2) is given by

$$\begin{cases} \dot{\xi}(t) = \Phi(t, \xi(t), \xi(t-\varsigma)) + \check{u}(t), \quad t \in (t_k, s_k), \\ \dot{\xi}(t) = \Phi(t, \xi(t), \xi(t-\varsigma)), \quad t \in [s_k, t_{k+1}), \\ \xi(t_k^+) = [(I_N - c\mathcal{H}) \otimes I_n]\xi(t_k^-) + c[\Omega(t_k) \otimes I_n]Q(t_k), t = t_k, \end{cases} \tag{3.8}$$

where $\xi(t) = \mathrm{col}(\xi_1(t), \xi_2(t), \ldots, \xi_N(t))$, and $\check{u}(t) = -c(\mathcal{H} \otimes I_n)\xi(t)$. Additionally, the composite nonlinear term takes the form: $\Phi(t, \xi(t), \xi(t-\varsigma)) = \mathrm{col}(\tilde{\mathfrak{R}}(t, \xi_i(t), \xi_i(t-\varsigma)))_{i=1}^N$.

Remark 3.2. *Deception attacks can distort the information received by followers and thereby deteriorate the consensus performance of the MAS. Because impulsive control updates are implemented at the triggering instants, incorporating the attack effect into the impulsive control law is essential for capturing the actual closed-loop behavior under malicious data injection. Moreover, introducing impulsive correction at these instants can effectively reduce the negative impact of attacked information and further improve the system stability and convergence behavior.*

Remark 3.3. *When no deception attack occurs, the injected attack signal satisfies* $Q(t_k) = 0$. *As a result, the attack-dependent term in* (3.8) *vanishes. In this specific case, our developed control framework simplifies to the conventional form without cyber-attacks. However, considering the increasing frequency and impact of cyber-attacks in real-world networked systems, ignoring such threats is impractical. Therefore, our proposed method, by explicitly incorporating deception attacks, offers a more robust and applicable solution for practical MASs.*

4. Main results

To analyze the stability of the piecewise impulsive system (3.8) with time delays, we first establish the following key lemma, which serves as the mathematical foundation for the proof of Theorem 4.1.

Lemma 4.1. *Consider a positive definite function* $\Psi(t)$ *that is continuously differentiable between impulsive instants and has well-defined left and right limits at each* t_k*:*

$$\begin{cases} \dot{\Psi}(t) \le -a_1\Psi(t) + a_2\Psi(t-\varsigma), \quad t \in (t_k, s_k), \\ \dot{\Psi}(t) \le a_3\Psi(t) + a_2\Psi(t-\varsigma), \quad t \in [s_k, t_{k+1}), \\ \Psi\left(t_k^+\right) \le e^{\mu}\Psi\left(t_k^-\right) + m, \quad t = t_k, \end{cases} \tag{4.1}$$

where $a_1, a_2, a_3 > 0$, $a_1 > a_2$, $0 < \mu < 1$, *and* $m \ge 0$. *Suppose that the triggering sequence satisfies* $T_{\min} = \inf_{k \in \mathbb{N}} \{t_{k+1} - t_k\} > 0$. *If Assumptions 3.1 and 3.2 and the condition*

$$\Delta = -r + \frac{r + a_3 + a_2}{T} + \frac{\mu + r\varsigma}{U_D} < 0$$

are satisfied, then the positive definite function $\Psi(t)$ *is ultimately bounded and satisfies*

$$\limsup_{t\to\infty} \Psi(t) \le \frac{me^{(r+a_2+a_3)\varkappa + (\mu + r\varsigma)\rho}}{1 - e^{\Delta T_{\min}}}.$$

Proof. Detailed derivations and proofs are provided in the Appendix.

Remark 4.1. *Assumptions 3.1 and 3.2 are timing conditions on the event-triggered intermittent-control sequence. Assumption 3.1 provides an upper bound on the number of intermittent-control intervals, and hence on the number of impulsive triggering instants, and Assumption 3.2 bounds the accumulated duration of the resting intervals. These two estimates, together with the condition* $\Delta < 0$*, where*

$$\Delta = -r + \frac{r + a_2 + a_3}{T} + \frac{\mu + r\varsigma}{U_D},$$

ensure that the decay during the working intervals dominates the growth during the resting intervals and at impulsive instants. This guarantees the ultimate boundedness of the Lyapunov function in Lemma 4.1.

Remark 4.2. *The proposed comparison model is sufficiently general and can recover several existing models as special cases by suitably choosing the parameters. Specifically, when* $\varsigma = 0$*, the time-delay term disappears, and the model reduces to the delay-free case studied in [34]; that is,*

$$\begin{cases} \dot{\Psi}(t) \le -a_1\Psi(t), & t \in (t_k, s_k), \\ \dot{\Psi}(t) \le a_3\Psi(t), & t \in [s_k, t_{k+1}), \\ \Psi\left(t_k^+\right) \le e^{\mu}\Psi\left(t_k^-\right) + m, & t = t_k. \end{cases} \tag{4.2}$$

It should be noted that the constant m in (4.1) *is introduced to characterize the additional effect caused by deception attacks. If no deception attack is considered, that is,* $m = 0$*, then the model becomes the attack-free delayed model investigated in [37], namely,*

$$\begin{cases} \dot{\Psi}(t) \le -a_1\Psi(t) + a_2\Psi(t-\varsigma), & t \in (t_k, s_k), \\ \dot{\Psi}(t) \le a_3\Psi(t) + a_2\Psi(t-\varsigma), & t \in [s_k, t_{k+1}), \\ \Psi\left(t_k^+\right) \le e^{\mu}\Psi\left(t_k^-\right), & t = t_k. \end{cases} \tag{4.3}$$

Moreover, when impulsive control is removed, the proposed model further degenerates into the intermittent-control model considered in [11], given by

$$\begin{cases} \dot{\Psi}(t) \le -a_1\Psi(t) + a_2\Psi(t-\varsigma), & t \in [t_k, t_k+\delta_k), \\ \dot{\Psi}(t) \le a_3\Psi(t) + a_2\Psi(t-\varsigma), & t \in [t_k+\delta_k, t_{k+1}). \end{cases}$$

Therefore, the proposed framework simultaneously incorporates time delays, deception attacks, intermittent control, and impulsive effects. This indicates that the obtained results extend and unify several related stability criteria in the existing literature.

Theorem 4.1. *Consider the delayed MASs* (2.1) *governed by the closed-loop intermittent impulsive system* (3.8)*. Suppose that the triggering sequence satisfies* $T_{\min} = \inf_{k\in\mathbb{N}}\{t_{k+1} - t_k\} > 0$*. Under Assumptions 2.1, 2.2, 3.1, and 3.2, if*

$$-r + \frac{r + a_2 + a_3}{T} + \frac{\mu + r\varsigma}{U_D} < 0, \tag{4.4}$$

then the considered MASs achieve leader-following mean-square quasiconsensus, and the ultimate consensus error bound is given by

$$\limsup_{t\to\infty} \mathbb{E}\{\|\xi(t)\|^2\} \leq \frac{\mathcal{B}}{\lambda_{\min}(P)},$$

where

$$\mathcal{B} = \frac{m e^{(r+a_2+a_3)\varkappa+(\mu+r\varsigma)\rho}}{1-e^{\Delta T_{\min}}}.$$

Proof. Consider

$$V(\xi(t)) = \sum_{i=1}^{N} p_i \xi_i^\top(t)\xi_i(t). \tag{4.5}$$

When $t \in (t_k, s_k)$, one has

$$\begin{aligned}\dot{V}(\xi(t)) &= 2\sum_{i=1}^{N} p_i \xi_i^\top(t)\left[\tilde{\mathfrak{R}}(t,\xi_i(t),\xi_i(t-\varsigma)) - c\sum_{j=1}^{N} h_{ij}\xi_j(t)\right]\\ &= 2\sum_{i=1}^{N} p_i\xi_i^\top(t)\tilde{\mathfrak{R}}(t,\xi_i(t),\xi_i(t-\varsigma)) - 2c\sum_{i=1}^{N}\sum_{j=1}^{N} p_i h_{ij}\xi_i^\top(t)\xi_j(t).\end{aligned} \tag{4.6}$$

By Assumption 2.2 and Young's inequality, one has

$$\begin{aligned}2\sum_{i=1}^{N} p_i\xi_i^\top(t)\tilde{\mathfrak{R}}(t,\xi_i(t),\xi_i(t-\varsigma)) &\leq 2\sum_{i=1}^{N} p_i\|\xi_i(t)\|\left[\gamma_1\|\xi_i(t)\| + \gamma_2\|\xi_i(t-\varsigma)\|\right]\\ &= (2\gamma_1+\gamma_2)V(\xi(t)) + \gamma_2 V(\xi(t-\varsigma)).\end{aligned} \tag{4.7}$$

Moreover,

$$-2c\sum_{i=1}^{N}\sum_{j=1}^{N} p_i h_{ij}\xi_i^\top(t)\xi_j(t) = -2c\,\xi^\top(t)(P\mathcal{H}\otimes I_n)\xi(t). \tag{4.8}$$

From Lemma 2.1,

$$-2c\,\xi^\top(t)(P\mathcal{H}\otimes I_n)\xi(t) = -2c\,\xi^\top(t)\left(\frac{P\mathcal{H}+\mathcal{H}^\top P}{2}\otimes I_n\right)\xi(t) \leq -2c\,\frac{\lambda_{\min}\left(\frac{P\mathcal{H}+\mathcal{H}^\top P}{2}\right)}{\lambda_{\max}(P)}V(\xi(t)). \tag{4.9}$$

Combining (4.7), (4.9), and (4.6) yields

$$\dot{V}(\xi(t)) \leq -a_1 V(\xi(t)) + a_2 V(\xi(t-\varsigma)), \tag{4.10}$$

where

$$a_1 = 2c\frac{\lambda_{\min}\left(\frac{P\mathcal{H}+\mathcal{H}^T P}{2}\right)}{\lambda_{\max}(P)} - 2\gamma_1 - \gamma_2,\quad a_2 = \gamma_2.$$

Similarly, when $t \in [s_k, t_{k+1})$, one has

$$\begin{aligned}\dot{V}(\xi(t)) &= 2\sum_{i=1}^{N} p_i \xi_i^\top(t)\tilde{\mathfrak{N}}(t, \xi_i(t), \xi_i(t-\varsigma)) \\ &\le 2\sum_{i=1}^{N} p_i\|\xi_i(t)\|(\gamma_1\|\xi_i(t)\| + \gamma_2\|\xi_i(t-\varsigma)\|) \\ &\le a_3 V(\xi(t)) + a_2 V(\xi(t-\varsigma)),\end{aligned} \tag{4.11}$$

where $a_3 = 2\gamma_1 + \gamma_2$. When $t = t_k$, one obtains

$$\xi(t_k^+) = M\xi(t_k^-) + \mathcal{R}(t_k), \tag{4.12}$$

where $M = (I_N - c\mathcal{H}) \otimes I_n, \mathcal{R}(t_k) = c[\Omega(t_k) \otimes I_n]Q(t_k)$. Thus, it follows that

$$\begin{aligned}\mathbb{E}\{V(\xi(t_k^+))\} &= \mathbb{E}\{\xi^\top(t_k^+)(P \otimes I_n)\xi(t_k^+)\} \\ &= \mathbb{E}\{[\xi^\top(t_k^-)M^\top + \mathcal{R}^\top(t_k)](P \otimes I_n)[M\xi(t_k^-) + \mathcal{R}(t_k)]\} \\ &= \mathbb{E}\{\xi^\top(t_k^-)M^\top(P \otimes I_n)M\xi(t_k^-)\} + \mathbb{E}\{\xi^\top(t_k^-)M^\top(P \otimes I_n)\mathcal{R}(t_k)\} \\ &\quad + \mathbb{E}\{\mathcal{R}^\top(t_k)(P \otimes I_n)M\xi(t_k^-)\} + \mathbb{E}\{\mathcal{R}^\top(t_k)(P \otimes I_n)\mathcal{R}(t_k)\}.\end{aligned} \tag{4.13}$$

For the quadratic term, one has

$$\begin{aligned}\mathbb{E}\{\xi^\top(t_k^-)M^\top(P \otimes I_n)M\xi(t_k^-)\} &= \mathbb{E}\{\xi^\top(t_k^-)[(I_N - c\mathcal{H}^\top) \otimes I_n](P \otimes I_n)[(I_N - c\mathcal{H}) \otimes I_n]\xi(t_k^-)\} \\ &= \mathbb{E}\{\xi^\top(t_k^-)[((I_N - c\mathcal{H}^\top)P(I_N - c\mathcal{H})) \otimes I_n]\xi(t_k^-)\} \\ &\le \sigma_{\max}^2(I_N - c\mathcal{H})\,\mathbb{E}\{V(\xi(t_k^-))\}.\end{aligned} \tag{4.14}$$

For the cross term, by Young's inequality, we obtain

$$\begin{aligned}&\mathbb{E}\{\xi^\top(t_k^-)M^\top(P \otimes I_n)\mathcal{R}(t_k)\} + \mathbb{E}\{\mathcal{R}^\top(t_k)(P \otimes I_n)M\xi(t_k^-)\} \\ &\le \epsilon\,\mathbb{E}\{\xi^\top(t_k^-)(P \otimes I_n)\xi(t_k^-)\} + \epsilon^{-1}\mathbb{E}\{\mathcal{R}^\top(t_k)(P \otimes I_n)MM^\top(P \otimes I_n)\mathcal{R}(t_k)\} \\ &\le \epsilon\,\mathbb{E}\{V(\xi(t_k^-))\} + \epsilon^{-1}c^2 q\lambda_{\max}(P)\sigma_{\max}^2[\Gamma^\top(I_N - c\mathcal{H})].\end{aligned} \tag{4.15}$$

For the remaining stochastic term, it follows that

$$\begin{aligned}\mathbb{E}\{\mathcal{R}^\top(t_k)(P \otimes I_n)\mathcal{R}(t_k)\} &= \mathbb{E}\{c^2 Q^\top(t_k)(\Omega^\top(t_k) \otimes I_n)(P \otimes I_n)(\Omega(t_k) \otimes I_n)Q(t_k)\} \\ &= c^2\mathbb{E}\{Q^\top(t_k)[\Omega^\top(t_k)P\Omega(t_k) \otimes I_n]Q(t_k)\} \\ &\le c^2 q\,\sigma_{\max}^2(\Gamma)\lambda_{\max}(P).\end{aligned} \tag{4.16}$$

Thus, we obtain

$$\begin{aligned}\mathbb{E}\{V(\xi(t_k^+))\} &\le (\sigma_{\max}^2(I_N - c\mathcal{H}) + \epsilon)\mathbb{E}\{V(\xi(t_k^-))\} + \epsilon^{-1}c^2 q\lambda_{\max}(P)\sigma_{\max}^2[\Gamma^\top(I_N - c\mathcal{H})] \\ &\quad + c^2 q\sigma_{\max}^2(\Gamma)\lambda_{\max}(P) \\ &\le e^{\mu}\mathbb{E}\{V(\xi(t_k^-))\} + m,\end{aligned} \tag{4.17}$$

where $\mu = \ln(\sigma_{\max}^2(I_N - c\mathcal{H}) + \epsilon)$, and $m = \epsilon^{-1}c^2 q\lambda_{\max}(P)\sigma_{\max}^2[\Gamma^\top(I_N - c\mathcal{H})] + c^2 q\sigma_{\max}^2(\Gamma)\lambda_{\max}(P)$.

It follows from the differential inequalities obtained over the working and resting intervals and the impulsive inequality at t_k that the Lyapunov function satisfies the three inequalities in Lemma 4.1. Moreover, Assumption 3.1 bounds the number of intermittent-control intervals and impulsive updates, whereas Assumption 3.2 bounds the accumulated duration of the resting intervals. Therefore, under

$$-r + \frac{r + a_2 + a_3}{T} + \frac{\mu + r\varsigma}{U_D} < 0,$$

all the conditions of Lemma 4.1 are satisfied.

By applying Lemma 4.1, it follows that $\mathbb{E}\{V(\xi(t))\}$ is ultimately bounded and satisfies

$$\limsup_{t\to\infty} \mathbb{E}\{V(\xi(t))\} \leq \mathcal{B}.$$

Moreover, because $\lambda_{\min}(P)\|\xi(t)\|^2 \leq V(\xi(t))$, one further obtains

$$\limsup_{t\to\infty} \mathbb{E}\{\|\xi(t)\|^2\} \leq \frac{1}{\lambda_{\min}(P)} \limsup_{t\to\infty} \mathbb{E}\{V(\xi(t))\} \leq \frac{\mathcal{B}}{\lambda_{\min}(P)}. \tag{4.18}$$

Hence, the delayed MASs (2.1) achieve mean-square quasiconsensus.

Theorem 4.2. *Under the ETM* (3.3)*, suppose that* $\eta > 0$*,* $\Lambda > 0$*, and* $a_2 + a_3 > 0$*. Then, the triggering instants satisfy* $t_{k+1} - t_k \geq h^*,\ k \in \mathbb{N}$*, where*

$$h^* = \min\left\{\frac{\eta}{a_2 + a_3}, \Lambda\right\} > 0.$$

Therefore, the ETM (3.3) *is Zeno-free.*

Proof. According to the triggering rule (3.3), the next triggering instant may be generated either by the event-triggering condition or by the forced-triggering rule. Therefore, we distinguish the following two cases.

Case 1: Suppose that the event-triggering condition is satisfied before the forced-triggering instant. Consider the resting interval $t \in [s_k, t_{k+1})$. From (4.11) and Lemma 2.3, one obtains

$$\mathbb{E}\{V(\xi(t))\} \leq \mathbb{E}\{V(\xi(s_k))\}e^{(a_2+a_3)(t-s_k)}. \tag{4.19}$$

Because t_{k+1} is generated by the event-triggering condition, one has

$$\mathbb{E}\{V(\xi(t_{k+1}))\} = \mathbb{E}\{V(\xi(t_k))\}e^{\eta}. \tag{4.20}$$

Moreover, $V(\xi(t))$ is nonincreasing on the working interval $[t_k, s_k)$, and hence,

$$\mathbb{E}\{V(\xi(s_k))\} \leq \mathbb{E}\{V(\xi(t_k))\}.$$

Setting $t = t_{k+1}$ in (4.19) and combining the resulting inequality with (4.20) yields $e^{(a_2+a_3)(t_{k+1}-s_k)} \geq e^{\eta}$, which implies

$$t_{k+1} - s_k \geq \frac{\eta}{a_2 + a_3}.$$

Because $w_k = s_k - t_k > 0$, it follows that

$$t_{k+1} - t_k = (t_{k+1} - s_k) + (s_k - t_k) \geq \frac{\eta}{a_2 + a_3} + w_k > \frac{\eta}{a_2 + a_3}. \tag{4.21}$$

Case 2: Suppose that the event-triggering condition remains unsatisfied before the forced-triggering instant. According to the check-period rule, the next triggering instant is given by $t_{k+1} = t_k + \Lambda$. Therefore,

$$t_{k+1} - t_k = \Lambda > 0.$$

Combining the above two cases yields $t_{k+1} - t_k \geq h^*$, where $h^* = \min\{\eta/(a_2 + a_3), \Lambda\} > 0$. Therefore, infinitely many triggering instants cannot accumulate within any finite time interval, and the ETM (3.3) is Zeno-free. Consequently,

$$T_{\min} = \inf_{k \in \mathbb{N}} \{t_{k+1} - t_k\} \geq h^* > 0.$$

Thus, the condition $T_{\min} > 0$ required in Lemma 4.1 and Theorem 4.1 is satisfied.

Remark 4.3. *Theorem 4.1 not only provides a theoretical criterion for ensuring the mean-square ultimate boundedness of the consensus error, but also yields a numerically checkable feasibility condition. Specifically, the key inequality*

$$-r + \frac{r + a_2 + a_3}{T} + \frac{\mu + r\varsigma}{U_D} < 0$$

explicitly relates the admissible control configuration to several interpretable quantities. In particular, the constants a_2 and a_3 are determined by the nonlinearity bounds γ_1 and γ_2, ς denotes the state-delay bound, and T and U_D characterize the temporal constraints associated with the intermittent control scheme. Moreover, the parameter μ reflects the influence of the impulsive control law and the network topology. Hence, once these quantities are estimated or specified, the feasibility of the proposed scheme can be checked directly. This provides practical guidance for parameter tuning and controller design in delayed MASs under cyber attacks.

5. Simulation

Numerical simulations are given to support the proposed method. Examples 5.1 and 5.2 illustrate the control performance for the delay-free and delayed cases, respectively, and Example 5.3 provides a Monte Carlo validation of the mean-square quasiconsensus result.

Example 5.1. In this example, a second-order leader-following MAS without delay is studied, where one leader communicates with six followers, and $\varsigma = 0$. Figure 2 depicts the corresponding communication graph, and it satisfies the leader-rooted spanning tree condition. In the numerical simulation, a step size of $h = 0.01$ s is employed, and the total simulation duration is set to 100 s. The agent dynamics are described by

$$\begin{cases} \dot{X}_{i1}(t) = X_{i2}(t), \\ \dot{X}_{i2}(t) = -0.1\sin(X_{i1}(t)) - 0.0001X_{i2}(t) + u_i(t), \end{cases} \qquad i = 1, \ldots, 6.$$

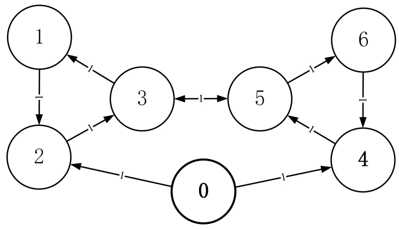

Figure 2. Directed communication topology.

The initial states of all agents are given by $\mathcal{X}_1(0) = [0.65, 0.5]^\top$, $\mathcal{X}_2(0) = [0.2, 0]^\top$, $\mathcal{X}_3(0) = [-0.5, 0.4]^\top$, $\mathcal{X}_4(0) = [0.3, 0]^\top$, $\mathcal{X}_5(0) = [0.35, 0]^\top$, $\mathcal{X}_6(0) = [0.8, 0.2]^\top$. Additionally, we configure the parameter matrix as $P = \text{diag}\{1.49, 1.46, 1.44, 1.41, 1.38, 1.37\} \in \mathbb{R}^{6\times6}$, which satisfies the condition in Lemma 2.1. With this choice, one obtains

$$\lambda_{\max}(P) = 1.49, \ \ \lambda_{\min}\left(\frac{P\mathcal{H} + \mathcal{H}^T P}{2}\right) = 0.309240, \ \text{ and } \ \sigma^2_{\max}(I_N - c\mathcal{H}) = 0.811745.$$

The control and event-triggering parameters are selected as $c = 0.5$, $\epsilon = 0.1883$, $\eta = 0.0001$, $w_k = 0.45$ s, and $\Lambda = 4$ s. The Lipschitz constants are chosen as $\gamma_1 = 0.10$ and $\gamma_2 = 0.0001$. Moreover, $||Q||^2 \leq 0.0001$, $T = 29$, and $U_D = 2$. The attack probability matrix is chosen as

$$\mathbb{E}[\Omega(t_k)] = \begin{bmatrix} 0 & 0 & 0.9 & 0 & 0 & 0 \\ 0.9 & 0 & 0.1 & 0 & 0.1 & 0 \\ 0 & 0.1 & 0 & 0.1 & 0.1 & 0 \\ 0.1 & 0 & 0.1 & 0 & 0.1 & 0.3 \\ 0.5 & 0.1 & 0.1 & 0.1 & 0 & 0 \\ 0 & 0 & 0.1 & 0 & 0.1 & 0 \end{bmatrix}.$$

By direct calculation, $a_1 = 0.007444$, $a_2 = 0.0001$, and $a_3 = 0.2001$, which satisfy $a_1 > a_2 > 0$. Because $\varsigma = 0$, one obtains $r = 0.007344$. Moreover, $\mu = 4.50 \times 10^{-5}$, which satisfies $0 < \mu < 1$. Furthermore,

$$\Delta = -r + \frac{r + a_2 + a_3}{T} + \frac{\mu + r\varsigma}{U_D} = -1.64 \times 10^{-4} < 0.$$

Thus, the theoretical conditions proposed in Theorem 4.1 are verified.

The numerical simulation outcomes are presented below. Figure 3 illustrates the follower-state trajectories under four cases: (a) the proposed ETM with a check-period subject to deception attacks, (b) the mechanism without a check-period [19] subject to attacks, (c) the detection-based mechanism [22] without attacks, and (d) the open-loop case. Comparing Figure 3(a) with Figure 3(b) reveals that the check-period Λ alleviates "silence events", enabling more timely updates and a faster convergence rate. Comparing Figure 3(a) with Figure 3(c) shows that subject to deception attacks, the proposed method preserves stable convergence behavior nearly identical to the attack-free baseline, which verifies its strong anti-attack capability. Figure 4 presents the 3-D error norms $||\xi_i(t)||$ for these four scenarios. Consistent with the trajectory results, Figure 4(a) exhibits a more rapid error decay than Figure 4(b) and closely tracks the attack-free trend of Figure 4(c). In contrast, Figure 4(d) shows persistent large oscillatory errors, providing additional evidence for the effectiveness of the proposed method.

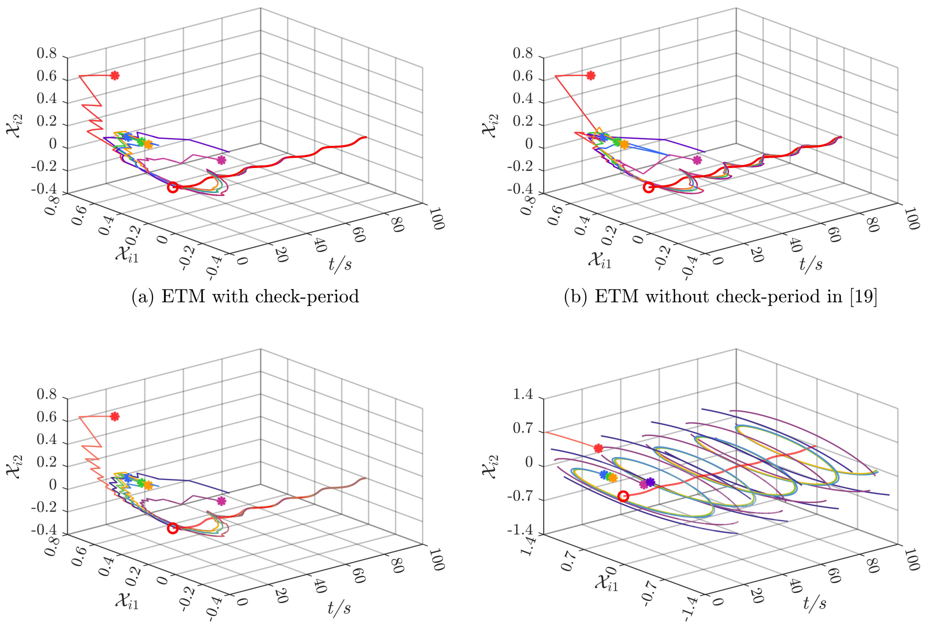

(a) ETM with check-period

(b) ETM without check-period in [19]

(c) Same as [22] without deception attacks

(d) No Control

Figure 3. State trajectories under different cases.

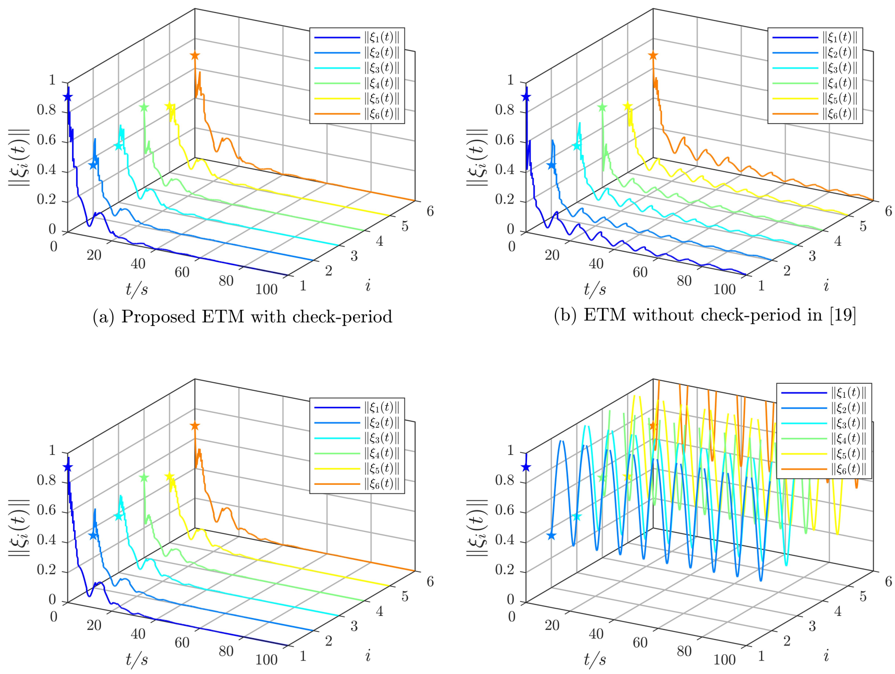

(a) Proposed ETM with check-period

(b) ETM without check-period in [19]

(c) Same as [22] without deception attacks

(d) No control

Figure 4. Error-norm trajectories $\|\xi_i(t)\|$ under different control strategies.

Figure 5 compares the interevent intervals Δt_k of the two scenarios, and Table 2 summarizes their total triggering numbers. The ETM without the check-period Λ in [19] is prone to causing "silence events", resulting in untimely system updates and thus requiring a longer convergence time. Conversely, the proposed check-period periodically verifies the triggering condition to prevent excessively long "silence intervals". As shown in Table 2, the proposed method generates 41 triggering instants, whereas the mechanism in [19] only produces 18 due to the occurrence of "silence events". Overall, the proposed method better achieves leader-following consensus subject to deception attacks. The additional triggering instants introduced by the check-period effectively suppress silence intervals and improve convergence performance, and the convergence behavior close to the attack-free case demonstrates strong robustness against deception attacks.

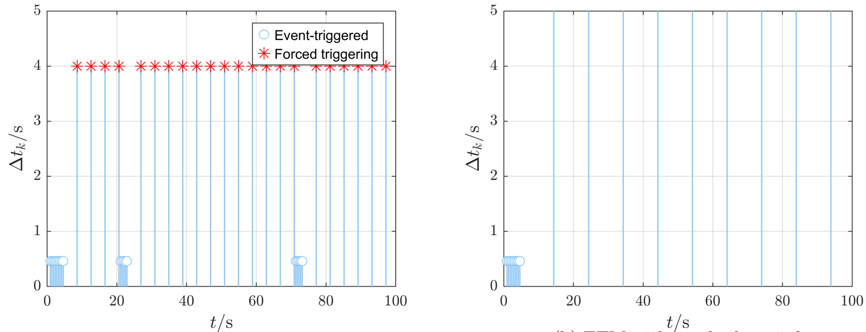

(a) ETM with check-period (b) ETM without check-period

Figure 5. Evolution of the interevent intervals Δt_k under the two ETMs.

Table 2. Total number of triggering instants for the two ETM settings.

Configuration	Total triggering instants
(a) ETM with check-period	41
(b) ETM without check-period in [19]	18

Example 5.2. This example considers a consensus control simulation model of second-order MASs with a state delay ($\varsigma = 0.05$ s). Based on the MASs formulated in (2.1) along with the directed graph shown in Figure 2, the step size for numerical simulations is fixed at $h = 0.01$ s, running for a total duration of $T_{total} = 100$ s. Each follower obeys the second-order linear dynamic equation, and its dynamic characteristics satisfy

$$\begin{cases} \dot{\mathcal{X}}_{i1}(t) = \mathcal{X}_{i2}(t), \\ \dot{\mathcal{X}}_{i2}(t) = -6.76\mathcal{X}_{i1}(t) - 0.0936\mathcal{X}_{i2}(t) + 0.02\mathcal{X}_{i1}(t-0.05) + 0.1\mathcal{X}_{i2}(t-0.05) + u_i(t). \end{cases} \quad i = 1, 2, \ldots, 6, \tag{5.1}$$

The initial states of each agent are assigned as follows: $x_0(0) = [0.02; 0]^\top$, $\mathcal{X}_1(0) = [0.15, 0.8]^\top$, $\mathcal{X}_2(0) = [0.2, 0.3]^\top$, $\mathcal{X}_3(0) = [0.25, 0.1]^\top$, $\mathcal{X}_4(0) = [-0.3, 0]^\top$, $\mathcal{X}_5(0) = [0.35, 0.3]^\top$, and $\mathcal{X}_6(0) = [-0.4, 0.5]^\top$; the same matrix P as in Example 5.1 is adopted. The key parameters are selected as follows:

$$c = 0.45,\ \epsilon = 0.18,\ \eta = 0.00001,\ \gamma_1 = 0.0002,\ \gamma_2 = 0.0009,$$

$$\Lambda = 3.5\text{ s},\ \|Q\|^2 \leq 0.0001,\ T = 1.13,\ \text{and } U_D = 1.6,$$

and the attack probability matrix is chosen as

$$\mathbb{E}[\Omega(t_k)] = \begin{bmatrix} 0 & 0 & 0.9 & 0 & 0 & 0 \\ 0.9 & 0 & 0.1 & 0 & 0.1 & 0 \\ 0 & 0.1 & 0 & 0.1 & 0.1 & 0 \\ 0.1 & 0 & 0.1 & 0 & 0.1 & 0.3 \\ 0.5 & 0.1 & 0.1 & 0.1 & 0 & 0 \\ 0 & 0 & 0.1 & 0 & 0.1 & 0 \end{bmatrix}.$$

Direct calculation gives

$$a_1 = 0.185489,\ a_2 = 0.0009,\ r = 0.184581,\ \mu = 0.006492,\ \Delta = -0.009462 < 0.$$

Thus, the theoretical conditions proposed in Theorem 4.1 are verified.

Simulation results are given below. Figure 6 compares the multi-agent trajectories under four strategies. With a check-period Λ, the proposed ETM in Figure 6(a) achieves fast convergence to the leader and preserves accurate tracking subject to deception attacks. Figure 6(b), the ETM without a check-period in [19], converges more slowly. Comparing Figure 6(a) with the attack-free baseline. Figure 6(c) shows that, subject to deception attacks, the proposed method retains nearly identical convergence behavior, demonstrating strong anti-attack capability. Without control in Figure 6(d), the agents fail to converge.

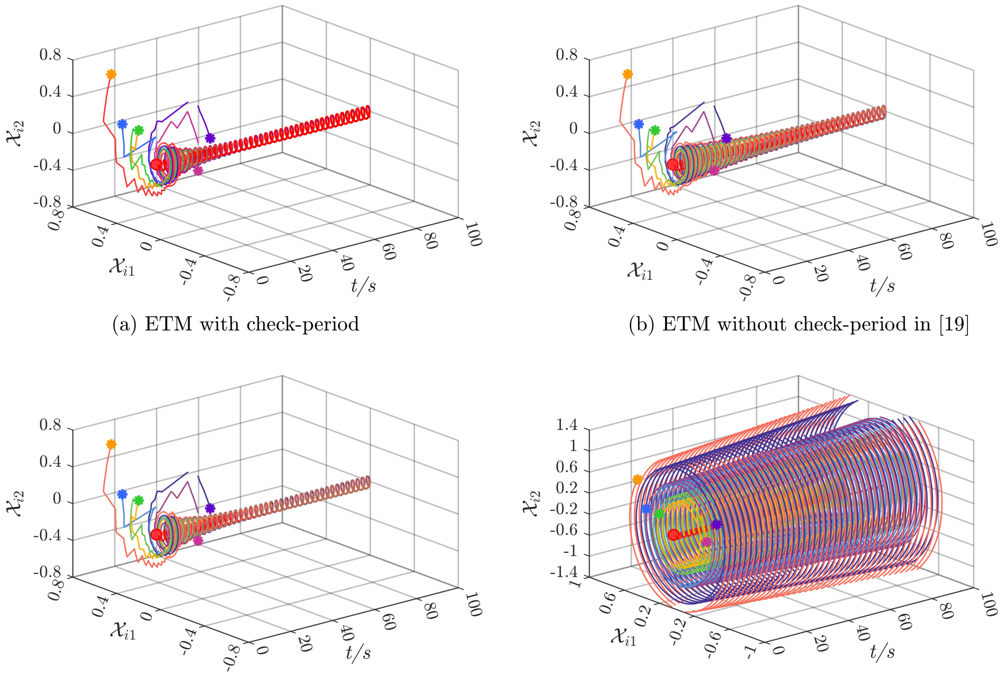

(a) ETM with check-period

(b) ETM without check-period in [19]

(c) Same as [22] without deception attacks

(d) No Control

Figure 6. Dynamic trajectories of agents under various control strategies.

Figure 7 shows the followers' error norms $\|\xi_i(t)\|$ for the same scenarios. The red dashed lines mark triggering instants. As expected, the proposed ETM in Figure 7(a) yields a faster error decay than the ETM without a check-period in Figure 7(b) and closely follows the attack-free trend in Figure 7(c). In contrast, no control in Figure 7(d) leads to persistent large oscillations.

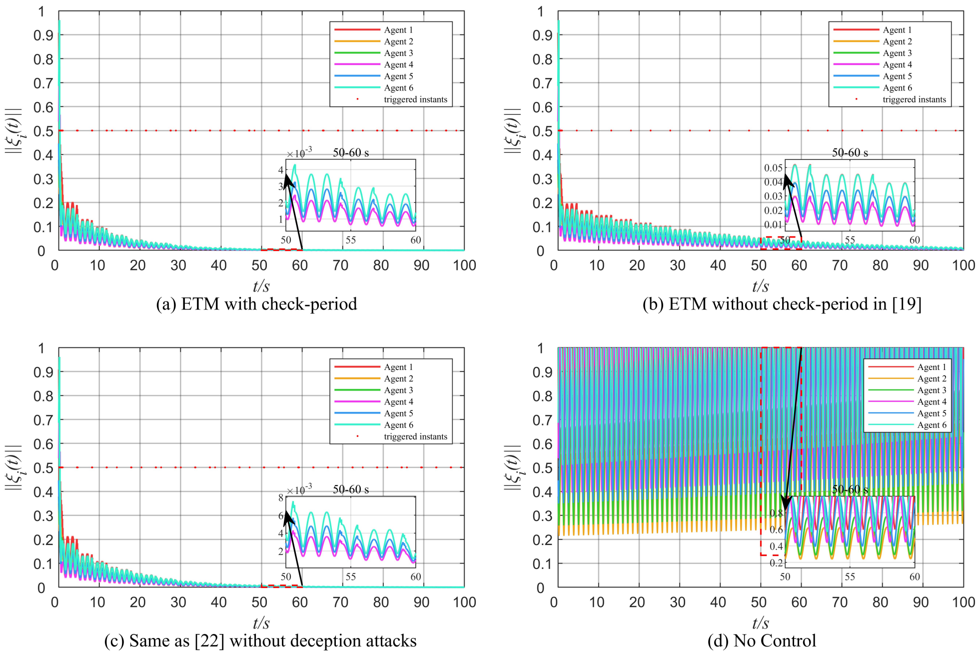

(a) ETM with check-period
(b) ETM without check-period in [19]
(c) Same as [22] without deception attacks
(d) No Control

Figure 7. Error norm trajectories $\|\xi_i(t)\|$ for agents under various control strategies.

Figure 8 compares the interevent times Δt_k of two ETMs. The proposed ETM with check-period Λ in Figure 8(a) distinguishes event-triggered updates and forced triggering, capping Δt_k at Λ to avoid long intervals. In contrast, the ETM without check-period in Figure 8(b) shows increasingly sparse triggering, leading to larger Δt_k and slower convergence due to silence events. Moreover, as demonstrated in Table 3, the proposed periodic-check ETM provides 66 triggering events, and the scheme in [19] without a check-period merely yields 30, which is mainly attributed to the emergence of "silence events".

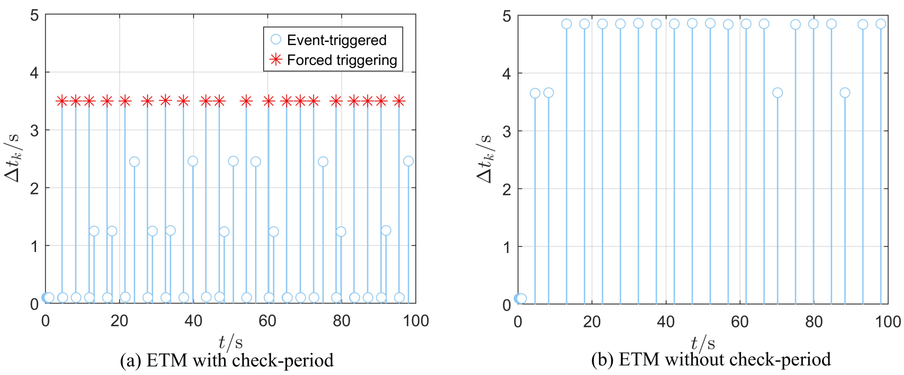

(a) ETM with check-period
(b) ETM without check-period

Figure 8. Evolution of trigger intervals Δt_k.

Table 3. Total number of triggering instants for the two ETM settings.

Configuration	Total triggering instants
(a) ETM with check-period	66
(b) ETM without check-period in [19]	30

Overall, under state delay conditions, the proposed check-period-enabled ETM achieves superior convergence speed, reliable anti-deception-attack performance, regular triggering behavior, and effective suppression of silence events compared with the existing ETM. Despite the state delay, the proposed method achieves a favorable balance between convergence and resource consumption, and its performance close to the attack-free case confirms strong robustness against deception attacks.

In the considered scheme, each triggering instant produces one communication update and one impulsive control action. The controller activation time is calculated as the accumulated duration of all working intervals. As shown in Table 4, the proposed method requires more triggering instants than the ETM without a check-period in [19]. However, these additional updates prevent excessively long silence intervals and provide more timely corrections of the consensus error.

Table 4. Overall comparison of convergence performance and resource consumption.

Example	Method	Check-period	Communication count	Impulse count	Controller activation time (s)	Main observation
Example 5.1	Proposed method	Yes	41	41	18.45	Faster convergence and suppression of silence intervals
Example 5.1	Ref. [19]	No	18	18	8.1	Sparse triggering and slower convergence
Example 5.1	Open-loop case	–	0	0	0	No consensus and persistent oscillatory errors
Example 5.2	Proposed method	Yes	66	66	6.6	Faster convergence subject to state delay
Example 5.2	Ref. [19]	No	30	30	3.0	Sparse triggering and slower convergence
Example 5.2	Open-loop case	–	0	0	0	No consensus and persistent large oscillations

Example 5.3. To further verify the mean-square quasiconsensus result, 500 independent Monte Carlo simulations are performed using the delayed multi-agent system, parameters, and initial conditions in Example 5.2. At each triggering instant, the attack variable of each agent is independently generated according to a Bernoulli distribution with attack probability 0.5 and is regenerated independently at different triggering instants. For the state delay $\varsigma = 0.05$ s, constant history functions are adopted, that is, $\xi_i(\theta) = \xi_i(0)$ for $\theta \in [-\varsigma, 0]$ and $i \in \mathcal{N}$.

At each sampling instant t_j, the Monte Carlo mean of the squared leader-following consensus errors obtained from the 500 independent attack realizations is calculated as

$$\overline{Z}(t_j) = \frac{1}{500} \sum_{q=1}^{500} \left\| \xi^{(q)}(t_j) \right\|^2 ,$$

where $\overline{Z}(t_j)$ denotes the average squared consensus error over the 500 Monte Carlo simulations. Table 5 summarizes the steady-state statistics over [80, 100] s.

Table 5. Statistical results of the 500 Monte Carlo realizations.

Statistical quantity	Value
Steady-state Monte Carlo mean of $\|\|\xi(t)\|\|^2$	1.3732×10^{-7}
Steady-state 95% CI of $\|\|\xi(t)\|\|^2$	$[1.3223 \times 10^{-7},\ 1.4240 \times 10^{-7}]$
Theoretical ultimate bound	3.4179×10^{-1}

Figure 9(a) shows the squared consensus error samples under the 500 independent attack realizations, their pointwise Monte Carlo mean, the 95% confidence region, and the theoretical ultimate bound. Figure 9(b) provides an enlarged view of the steady-state responses over [80, 85] s, and the interval [80, 100] s is used to calculate the steady-state statistics. According to Theorem 4.1, the theoretical ultimate bound of $\mathbb{E}\{||\xi(t)||^2\}$ is 3.4179×10^{-1}. The steady-state Monte Carlo mean is 1.3732×10^{-7}, and its 95% confidence interval is $[1.3223 \times 10^{-7}, 1.4240 \times 10^{-7}]$, both of which are far below the theoretical bound. Therefore, the Monte Carlo results provide further numerical support for the mean-square leader-following quasiconsensus result. The gap between the simulated errors and the theoretical bound is mainly attributed to the conservative worst-case estimates adopted in the Lyapunov analysis.

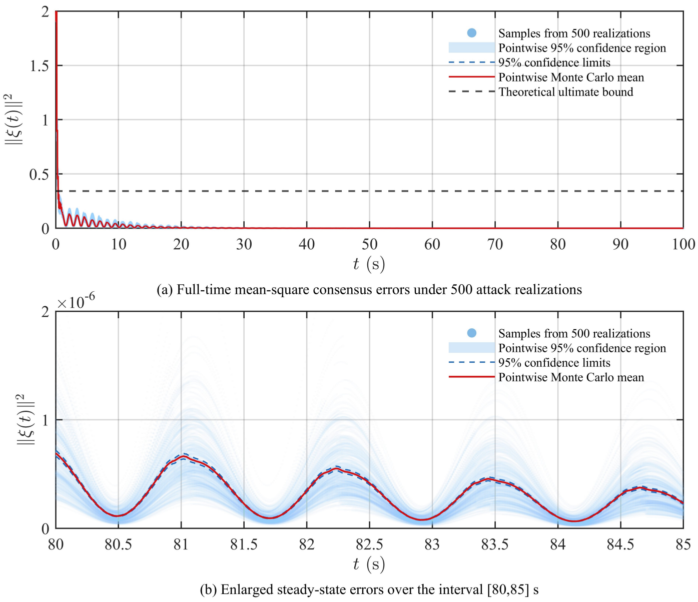

Figure 9. Monte Carlo results under 500 independent deception-attack realizations.

6. Conclusions

This work addresses mean-square quasiconsensus for delayed leader-following MASs in the presence of deception attacks by utilizing an impulsive control that relies on an ETM. First, a closed-loop intermittent control has been developed where the start of the operational window is determined dynamically via a Lyapunov function-based ETM according to current system states. Then, a new piecewise differential inequality incorporating state delays has been formulated to address the challenges arising from the combination of state-dependent intermittent control, time delays in states, deceptive attacks, and impulsive control. Furthermore, a sufficient criterion has been formulated to realize mean-square quasiconsensus of delayed MASs against deception attacks. Finally, simulation results have been provided to confirm the feasibility of the theoretical framework. Because most of the group behaviors in real environments are heterogeneous, such as machine vehicle collaboration and machine ship collaboration, future research will primarily focus on the cooperative control of heterogeneous MASs suffering from combined cyber attacks.

Author contributions

Chen Liu: Writing–review & editing, Writing–original draft, Validation, Software, Methodology, Conceptualization; Mengting Wang, Qing Chen and Yihao Chu: Writing–review & editing, Validation. All authors have read and approved the final version of the manuscript for publication.

Use of Generative-AI tools declaration

The authors declare they have not used Artificial Intelligence (AI) tools in the creation of this article.

Acknowledgments

This work was supported in part by the Tianyuan Fund for Mathematics of the National Natural Science Foundation of China under Grant 12526633; and in part by the Anhui Provincial University Research Plan Projects of China under Grant 2025AHGXZK30807.

Conflict of interest

The authors declare that no known competing financial interests or personal relationships are associated with the work presented in this paper.

References

1. Y. S. Zheng, J. Y. Ma, L. Wang, Consensus of hybrid multi-agent systems, *IEEE Trans. Neural Netw. Learn. Syst.*, **29** (2018), 1359–1365. https://doi.org/10.1109/TNNLS.2017.2651402
2. X. W. Dong, B. C. Yu, Z. Y. Shi, Y. S. Zhong, Time-varying formation control for unmanned aerial vehicles: theories and applications, *IEEE Trans. Control Syst. Technol.*, **23** (2015), 340–348. https://doi.org/10.1109/tcst.2014.2314460
3. R. Z. Homod, Z. M. Yaseen, A. K. Hussein, A. Almusaed, O. A. Alawi, M. W. Falah, et al., Deep clustering of cooperative multi-agent reinforcement learning to optimize multi chiller HVAC systems for smart buildings energy management, *J. Build. Eng.*, **65** (2023), 105689. https://doi.org/10.1016/j.jobe.2022.105689

4. L. Schenato, F. Fiorentin, Average TimeSynch: a consensus-based protocol for clock synchronization in wireless sensor networks, *Automatica*, **47** (2011), 1878–1886. https://doi.org/10.1016/j.automatica.2011.06.012

5. Z. W. Yan, L. Han, X. D. Li, X. W. Dong, Q. D. Li, Z. Ren, Event-triggered formation control for time-delayed discrete-time multi-agent system applied to multi-UAV formation flying, *J. Franklin Inst.*, **360** (2023), 3677–3699. https://doi.org/10.1016/j.jfranklin.2023.01.036

6. O. P. Mahela, M. Khosravy, N. Gupta, B. Khan, H. H. Alhelou, R. Mahla, et al., Comprehensive overview of multi-agent systems for controlling smart grids, *CSEE J. Power Energy Syst.*, **8** (2022), 115–131. https://doi.org/10.17775/cseejpes.2020.03390

7. J. Y. Xu, J. X. Dong, Global prescribed performance bipartite consensus for linear multi-agent systems: a time-varying BLF-based gain method, *J. Franklin Inst.*, **362** (2025), 108102. https://doi.org/10.1016/j.jfranklin.2025.108102

8. Z. Y. Yu, H. J. Jiang, C. Hu, Second-order consensus for multiagent systems via intermittent sampled-data control, *IEEE Trans. Syst. Man Cybernet. Syst.*, **48** (2018), 1986–2002. https://doi.org/10.1109/tsmc.2017.2687944

9. S. C. He, X. D. Liu, P. L. Lu, C. K. Du, H. K. Liu, Distributed finite-time consensus algorithm for multiagent systems via aperiodically intermittent protocol, *IEEE Trans. Circuits Syst. II Express Briefs*, **69** (2022), 3229–3233. https://doi.org/10.1109/tcsii.2021.3135866

10. Y. Guo, Y. Qian, P. F. Wang, Leader-following consensus of delayed multi-agent systems with aperiodically intermittent communications, *Neurocomputing*, **466** (2021), 49–57. https://doi.org/10.1016/j.neucom.2021.09.014

11. J. F. Wang, Z. Tang, D. Ding, J. W. Feng, Aperiodically intermittent saturation consensus on multi-agent systems with discontinuous dynamics, *ISA Trans.*, **133** (2023), 66–74. https://doi.org/10.1016/j.isatra.2022.06.031

12. J. R. Xiao, Y. F. Hu, X. Y. Liu, J. D. Cao, Bipartite consensus of second-order delayed unknown multi-agent systems via aperiodically intermittent control, *Asian J. Control*, **27** (2025), 2530–2540. https://doi.org/10.1002/asjc.3605

13. L. Ding, Q. L. Han, X. H. Ge, X. M. Zhang, An overview of recent advances in event-triggered consensus of multiagent systems, *IEEE Trans. Cybernet.*, **48** (2018), 1110–1123. https://doi.org/10.1109/tcyb.2017.2771560

14. D. V. Dimarogonas, E. Frazzoli, K. H. Johansson, Distributed event-triggered control for multi-agent systems, *IEEE Trans. Autom. Control*, **57** (2012), 1291–1297. https://doi.org/10.1109/tac.2011.2174666

15. D. S. Xie, S. Y. Xu, Y. M. Chu, Y. Zou, Event-triggered average consensus for multi-agent systems with nonlinear dynamics and switching topology, *J. Franklin Inst.*, **352** (2015), 1080–1098. https://doi.org/10.1016/j.jfranklin.2014.11.004

16. M. Zhao, C. Peng, W. L. He, Y. Song, Event-triggered communication for leader-following consensus of second-order multiagent systems, *IEEE Trans. Cybernet.*, **48** (2018), 1888–1897. https://doi.org/10.1109/tcyb.2017.2716970

17. L. C. Zhang, Y. R. Li, C. K. Ahn, H. J. Liang, Adaptive temporal partitioning for communication-efficient consensus in nonlinear multiagent systems, *IEEE Trans. Ind. Inform.*, 2026, 1–12. https://doi.org/10.1109/TII.2026.3709625
18. Y. N. Pan, Y. L. Chen, H. J. Liang, Event-triggered predefined-time control for full-state constrained nonlinear systems: a novel command filtering error compensation method, *Sci. China Technol. Sci.*, **67** (2024), 2867–2880. https://doi.org/10.1007/s11431-023-2607-8
19. A. H. Hu, J. H. Park, M. F. Hu, Consensus of nonlinear multiagent systems with intermittent dynamic event-triggered protocols, *Nonlinear Dyn.*, **104** (2021), 1299–1313. https://doi.org/10.1007/s11071-021-06321-6
20. H. J. Liang, Z. Y. Chang, C. K. Ahn, Hybrid event-triggered intermittent control for nonlinear multi-agent systems, *IEEE Trans. Netw. Sci. Eng.*, **10** (2023), 1975–1984. https://doi.org/10.1109/tnse.2023.3237256
21. C. Liu, L. Liu, Z. J. Wu, Intermittent event-triggered optimal control for second-order delayed multiagent systems with input constraints, *IEEE Trans. Syst. Man Cybernet. Syst.*, **54** (2024), 2698–2710. https://doi.org/10.1109/tsmc.2023.3346949
22. X. F. Zhu, Z. Tang, J. W. Feng, J. H. Park, Aperiodically intermittent event-triggered pinning control on cluster synchronization of directed complex networks, *ISA Trans.*, **138** (2023), 281–290. https://doi.org/10.1016/j.isatra.2023.02.027
23. B. Liu, T. Liu, P. Xiao, Dynamic event-triggered intermittent control for stabilization of delayed dynamical systems, *Automatica*, **149** (2023), 110847. https://doi.org/10.1016/j.automatica.2022.110847
24. Z. H. Ma, D. Ding, Z. Tang, Containment control for non-linear multi-agent systems under distributed event-triggering intermittent schemes, *Int. J. Robust Nonlinear Control*, **35** (2025), 3751–3762. https://doi.org/10.1002/rnc.7879
25. T. D. Ma, K. Li, Z. L. Zhang, B. Cui, Impulsive consensus of one-sided Lipschitz nonlinear multi-agent systems with semi-Markov switching topologies, *Nonlinear Anal. Hybrid Syst.*, **40** (2021), 101020. https://doi.org/10.1016/j.nahs.2021.101020
26. W. Y. Tang, C. J. Liang, J. Wu, Y. F. Xie, Distributed impulsive control consensus for a class of unknown nonlinear multi-agent systems based on event-triggered scheme, *Nonlinear Anal. Hybrid Syst.*, **49** (2023), 101352. https://doi.org/10.1016/j.nahs.2023.101352
27. X. Wang, S. D. Wang, J. Liu, Y. B. Wu, C. Y. Sun, Bipartite finite-time consensus of multi-agent systems with intermittent communication via event-triggered impulsive control, *Neurocomputing*, **598** (2024), 127970. https://doi.org/10.1016/j.neucom.2024.127970
28. K. P. Wang, D. Ding, Z. Tang, J. W. Feng, Leader-following consensus of nonlinear multi-agent systems with hybrid delays: distributed impulsive pinning strategy, *Appl. Math. Comput.*, **424** (2022), 127031. https://doi.org/10.1016/j.amc.2022.127031
29. Y. L. Wang, J. D. Cao, H. J. Wang, Event-based impulsive consensus for delayed multi-agent systems, *Asian J. Control*, **24** (2022), 771–781. https://doi.org/10.1002/asjc.2646
30. F. H. Zhang, C. L. Zhan, T. W. Huang, Z. G. Zeng, Synchronization of delayed complex networks via event-triggered intermittent impulsive control, *J. Franklin Inst.*, **362** (2025), 108109. https://doi.org/10.1016/j.jfranklin.2025.108109

31. W. L. He, W. Y. Xu, X. H. Ge, Q. L. Han, W. L. Du, F. Qian, Secure control of multiagent systems against malicious attacks: a brief survey, *IEEE Trans. Ind. Inform.*, **18** (2022), 3595–3608. https://doi.org/10.1109/tii.2021.3126644

32. G. D. Zong, H. Z. Xie, D. Yang, X. D. Zhao, Y. Yi, Adaptive fuzzy tracking control for switched nonlinear systems under FDI attacks and input saturation: a flexible transient performance approach, *IEEE Trans. Cybernet.*, **54** (2024), 7479–7488. https://doi.org/10.1109/TCYB.2024.3463689

33. T. T. Yin, Z. Gu, J. H. Park, Event-based intermittent formation control of multi-UAV systems under deception attacks, *IEEE Trans. Neural Netw. Learn. Syst.*, **35** (2024), 8336–8347. https://doi.org/10.1109/tnnls.2022.3227101

34. Z. W. Liu, Y. L. Shi, H. C. Yan, B. X. Han, Z. H. Guan, Secure consensus of multiagent systems via impulsive control subject to deception attacks, *IEEE Trans. Circuits Syst. II Express Briefs*, **70** (2023), 166–170. https://doi.org/10.1109/tcsii.2022.3196042

35. C. Zhao, X. Z. Liu, S. M. Zhong, K. B. Shi, D. X. Liao, Q. S. Zhong, Secure consensus of multi-agent systems with redundant signal and communication interference via distributed dynamic event-triggered control, *ISA Trans.*, **112** (2021), 89–98. https://doi.org/10.1016/j.isatra.2020.11.030

36. X. T. Zhou, J. Q. Tan, L. L. Li, Y. Yao, H. H. Zhang, Secure synchronization of stochastic neural networks under deception attacks: an event-based intermittent impulsive approach, *Neurocomputing*, **654** (2025), 131271. https://doi.org/10.1016/j.neucom.2025.131271

37. Y. N. Wang, C. D. Li, H. J. Wu, H. Deng, Stabilization of nonlinear delayed systems subject to impulsive disturbance via aperiodic intermittent control, *J. Franklin Inst.*, **361** (2024), 106675. https://doi.org/10.1016/j.jfranklin.2024.106675

38. X. G. Tan, J. D. Cao, X. D. Li, Consensus of leader-following multiagent systems: a distributed event-triggered impulsive control strategy, *IEEE Trans. Cybernet.*, **49** (2019), 792–801. https://doi.org/10.1109/tcyb.2017.2786474

39. E. N. Sanchez, J. P. Perez, Input-to-state stability (ISS) analysis for dynamic neural networks, *IEEE Trans. Circuits Syst. I Fundam. Theory Appl.*, **46** (1999), 1395–1398. https://doi.org/10.1109/81.802844

40. J. Bebernes, Differential equations stability, oscillations, time lags (A. Halanay), *SIAM Rev.*, **10** (1968), 93–94. https://doi.org/10.1137/1010009

41. C. D. Li, X. F. Liao, T. W. Huang, Exponential stabilization of chaotic systems with delay by periodically intermittent control, *Chaos*, **17** (2007), 013103. https://doi.org/10.1063/1.2430394

42. W. L. He, X. Y. Gao, W. M. Zhong, F. Qian, Secure impulsive synchronization control of multi-agent systems under deception attacks, *Inform. Sci.*, **459** (2018), 354–368. https://doi.org/10.1016/j.ins.2018.04.020

43. Y. Zhai, P. F. Wang, H. Su, Stabilization of stochastic complex networks with delays based on completely aperiodically intermittent control, *Nonlinear Anal. Hybrid Syst.*, **42** (2021), 101074. https://doi.org/10.1016/j.nahs.2021.101074

Appendix

Proof of Lemma 4.1. Because $\Psi(t)$ may be discontinuous at each impulsive instant t_k, define $\Psi(t_k^-) = \lim_{t\to t_k^-}\Psi(t)$ and $\Psi(t_k^+) = \lim_{t\to t_k^+}\Psi(t)$. To incorporate the delayed history and the post-impulsive value, define $\tilde{\Psi}(t) = \sup_{t-\varsigma\le\theta\le t}\Psi(\theta)$ at a continuous instant t, and $\tilde{\Psi}(t_k^+) = \max\left\{\Psi(t_k^+), \sup_{t_k-\varsigma\le\theta<t_k}\Psi(\theta)\right\}$ at an impulsive instant t_k. Because $\Psi(t_k^-) \le \tilde{\Psi}(t_k^-)$, and $\sup_{t_k-\varsigma\le\theta<t_k}\Psi(\theta) \le \tilde{\Psi}(t_k^-)$, the impulsive inequality gives

$$\tilde{\Psi}(t_k^+) \le \max\left\{e^{\mu}\Psi(t_k^-) + m, \tilde{\Psi}(t_k^-)\right\} \le e^{\mu}\tilde{\Psi}(t_k^-) + m,$$

where the last inequality follows from $e^{\mu} > 1$ and $m \ge 0$. Thus, the impulsive estimate simultaneously includes the post-impulsive value and the delayed history preceding t_k.

When $t \in [t_0, s_0)$, it follows that

$$\begin{cases}\Psi(t) \le \tilde{\Psi}(t_0)e^{-r(t-t_0)},\\ \tilde{\Psi}(s_0) = \sup\limits_{s_0-\varsigma\le\theta\le s_0}\Psi(\theta) \le \tilde{\Psi}(t_0)e^{-r(s_0-\varsigma-t_0)},\end{cases} \tag{6.1}$$

when $t \in [s_0, t_1)$,

$$\begin{cases}\Psi(t) \le \tilde{\Psi}(s_0)e^{(a_2+a_3)(t-s_0)} \le \tilde{\Psi}(t_0)e^{-r(s_0-\varsigma-t_0)+(a_2+a_3)(t-s_0)},\\ \Psi(t_1^-) \le \tilde{\Psi}(t_0)e^{-r(s_0-\varsigma-t_0)+(a_2+a_3)(t_1^--s_0)}.\end{cases} \tag{6.2}$$

According to $\tilde{\Psi}(t_k^+) \le e^{\mu}\tilde{\Psi}(t_k^-) + m$, at $t = t_1$, one obtains

$$\tilde{\Psi}(t_1^+) \le e^{\mu}\tilde{\Psi}(t_1^-) + m \le e^{\mu}\tilde{\Psi}(t_0^+)e^{-r(s_0-\varsigma-t_0)+(a_2+a_3)(t_1^--s_0)} + m.$$

When $t \in (t_1, s_1)$,

$$\begin{cases}\Psi(t) \le \tilde{\Psi}(t_1^+)e^{-r(t-t_1)} \le \left(e^{\mu}\tilde{\Psi}(t_0)e^{-r(s_0-\varsigma-t_0)+(a_2+a_3)(t_1^--s_0)} + m\right)e^{-r(t-t_1)},\\ \tilde{\Psi}(s_1) = \sup\limits_{s_1-\varsigma\le\theta\le s_1}\Psi(\theta) = e^{\mu}\tilde{\Psi}(t_0)e^{-r(s_0-\varsigma-t_0)-r(s_1-\varsigma-t_1)+(a_2+a_3)(t_1^--s_0)} + me^{-r(s_1-\varsigma-t_1)}.\end{cases} \tag{6.3}$$

When $t \in [s_1, t_2)$,

$$\begin{cases}\Psi(t) \le \tilde{\Psi}(s_1)e^{(a_2+a_3)(t-s_1)}\\ \qquad \le e^{\mu}\tilde{\Psi}(t_0)e^{-r(s_0-\varsigma-t_0)-r(s_1-\varsigma-t_1)+(a_2+a_3)(t_1^--s_0)+(a_2+a_3)(t-s_1)} + me^{-r(s_1-\varsigma-t_1)+(a_2+a_3)(t-s_1)},\\ \Psi(t_2^-) \le e^{\mu}\tilde{\Psi}(t_0)e^{-r\left[\sum_{i=1}^{2}(s_{i-1}-\varsigma-t_{i-1})\right]+(a_2+a_3)\left[\sum_{i=1}^{2}(t_i^--s_{i-1})\right]} + me^{-r(s_1-\varsigma-t_0)+(a_2+a_3)(t_2^--s_1)}.\end{cases} \tag{6.4}$$

Similarly, when $t = t_2$, it follows that

$$\begin{aligned}\tilde{\Psi}(t_2^+) &\le e^{\mu}\tilde{\Psi}(t_2^-) + m\\ &\le e^{2\mu}\tilde{\Psi}(t_0)e^{-r(s_0-\varsigma-t_0)-r(s_1-\varsigma-t_1)+(a_2+a_3)(t_1^--s_0)+(a_2+a_3)(t_2^--s_1)} + e^{\mu}me^{-r(s_1-\varsigma-t_0)+(a_2+a_3)(t_2^--s_1)} + m.\end{aligned} \tag{6.5}$$

Based on the above recurrence, it can be shown by mathematical induction that when $t = t_k$, which yields

$$
\begin{aligned}
\tilde{\Psi}(t_k^+) &\le e^{\mu}\tilde{\Psi}(t_k^-) + m \\
&\le \tilde{\Psi}(t_0)e^{k\mu - r\sum_{i=1}^{k}(s_{i-1}-\varsigma-t_{i-1})+\sum_{i=1}^{k}(a_2+a_3)(t_i^- - s_{i-1})} + m\sum_{n=1}^{k} e^{(k-n)\mu - r\sum_{i=n+1}^{k}(s_{i-1}-\varsigma-t_{i-1})+\sum_{i=n+1}^{k}(a_2+a_3)(t_i^- - s_{i-1})} \\
&= \tilde{\Psi}(t_0)e^{\mathcal{F}_1} + m\sum_{n=1}^{k} e^{\mathcal{F}_2},
\end{aligned} \tag{6.6}
$$

where $\mathcal{F}_1 = k\mu - r\sum_{i=1}^{k}(s_{i-1} - \varsigma - t_{i-1}) + \sum_{i=1}^{k}(a_2 + a_3)(t_i^- - s_{i-1})$, and $\mathcal{F}_2 = (k-n)\mu - r\sum_{i=n+1}^{k}(s_{i-1} - \varsigma - t_{i-1}) + \sum_{i=n+1}^{k}(a_2 + a_3)(t_i^- - s_{i-1})$, by Assumptions 3.1 and 3.2, one has

$$
\sum_{i=n+1}^{k}(t_i^- - s_{i-1}) \le \varkappa + \frac{t_k - t_n}{T}, \quad k - n \le \rho + \frac{t_k - t_n}{U_D}.
$$

Hence, we can obtain

$$
\begin{aligned}
\mathcal{F}_2 &\le (\mu + r\varsigma)(k-n) - r\sum_{i=n+1}^{k}(s_{i-1} - t_{i-1}) + (a_2 + a_3)\sum_{i=n+1}^{k}(t_i^- - s_{i-1}) \\
&\le \Delta(t_k - t_n) + (r + a_2 + a_3)\varkappa + (\mu + r\varsigma)\rho,
\end{aligned} \tag{6.7}
$$

where

$$
\Delta = \frac{\mu + r\varsigma}{U_D} - r + \frac{r + a_2 + a_3}{T} < 0.
$$

Suppose that the minimum interevent time satisfies $T_{\min} = \inf_{k\in\mathbb{N}}\{t_{k+1} - t_k\} > 0$. Then, for $1 \le n \le k$, one has

$$
t_k - t_n = \sum_{i=n}^{k-1}(t_{i+1} - t_i) \ge (k-n)T_{\min}.
$$

Because $\Delta < 0$, one has $e^{\Delta(t_k - t_n)} \le e^{\Delta(k-n)T_{\min}}$. Therefore,

$$
\sum_{n=1}^{k} e^{\Delta(t_k - t_n)} \le \sum_{n=1}^{k} e^{\Delta(k-n)T_{\min}} = \sum_{j=0}^{k-1} e^{j\Delta T_{\min}} = \frac{1 - e^{k\Delta T_{\min}}}{1 - e^{\Delta T_{\min}}}.
$$

Consequently, it holds that

$$
m\sum_{n=1}^{k} e^{\mathcal{F}_2} \le m e^{(r+a_2+a_3)\varkappa + (\mu+r\varsigma)\rho}\sum_{n=1}^{k} e^{\Delta(t_k - t_n)} \le m e^{(r+a_2+a_3)\varkappa + (\mu+r\varsigma)\rho}\frac{1 - e^{k\Delta T_{\min}}}{1 - e^{\Delta T_{\min}}}. \tag{6.8}
$$

Because $T_{\min} > 0$, and $\Delta < 0$, it holds that $0 < e^{\Delta T_{\min}} < 1$. Consequently, it obtains the ultimate bound for the second term:

$$
\lim_{k\to\infty} m\sum_{n=1}^{k} e^{\mathcal{F}_2} \le \frac{m e^{(r+a_2+a_3)\varkappa + (\mu+r\varsigma)\rho}}{1 - e^{\Delta T_{\min}}}. \tag{6.9}
$$

From Assumptions 3.1 and 3.2, we have

$$\sum_{i=1}^{k}(t_i^- - s_{i-1}) \le \varkappa + \frac{t_k - t_0}{T} \text{ and } k \le \rho + \frac{t_k - t_0}{U_D}.$$

Thus, this gives

$$\begin{aligned}\mathcal{F}_1 &\le k(\mu + r\varsigma) - r(t_k - t_0) + (r + a_2 + a_3)\sum_{i=1}^{k}(t_i^- - s_{i-1}) \\ &\le (\mu + r\varsigma)\left(\rho + \frac{t_k - t_0}{U_D}\right) - r(t_k - t_0) + (r + a_2 + a_3)\left(\varkappa + \frac{t_k - t_0}{T}\right) \\ &= \Delta(t_k - t_0) + (r + a_3 + a_2)\varkappa + (\mu + r\varsigma)\rho. \end{aligned} \tag{6.10}$$

Then, as a result,

$$e^{\mathcal{F}_1} \le e^{\Delta(t_k - t_0) + (r + a_3 + a_2)\varkappa + (\mu + r\varsigma)\rho}. \tag{6.11}$$

Because $\Delta < 0$, and $\lim_{k\to\infty} t_k = \infty$, we easily deduce that $\lim_{k\to\infty} e^{\mathcal{F}_1} = 0$. Therefore, according to (6.5), (6.9) and (6.11), the limit superior of the Lyapunov function at the impulsive triggering instants is bounded by

$$\limsup_{k\to\infty} \tilde{\Psi}(t_k^+) \le \frac{me^{(r+a_2+a_3)\varkappa + (\mu + r\varsigma)\rho}}{1 - e^{\Delta T_{\min}}}. \tag{6.12}$$

For any sufficiently large t, one can choose a sufficiently large integer k such that $t \in [t_k, t_{k+1})$. We distinguish the following two scenarios.

Case 1: $t \in [t_k, s_k)$. From the dynamics over the working interval, one has

$$\Psi(t) \le \tilde{\Psi}(t_k^+)e^{-r(t-t_k)}.$$

Substituting the iterative estimate of $\tilde{\Psi}(t_k^+)$ into the above inequality gives

$$\Psi(t) \le \tilde{\Psi}(t_0^+)e^{\Delta(t-t_0)+(r+a_2+a_3)\varkappa + (\mu + r\varsigma)\rho} + me^{(r+a_2+a_3)\varkappa+(\mu+r\varsigma)\rho}\sum_{n=1}^{k} e^{\Delta(t-t_n)}.$$

Because $t \ge t_k$, for $1 \le n \le k$,

$$t - t_n \ge t_k - t_n \ge (k - n)T_{\min}.$$

Because $\Delta < 0$, it follows that

$$\sum_{n=1}^{k} e^{\Delta(t-t_n)} \le \sum_{n=1}^{k} e^{\Delta(k-n)T_{\min}} \le \frac{1}{1 - e^{\Delta T_{\min}}}.$$

Hence,

$$\Psi(t) \le \tilde{\Psi}(t_0^+)e^{\Delta(t-t_0)+(r+a_2+a_3)\varkappa+(\mu+r\varsigma)\rho} + \frac{me^{(r+a_2+a_3)\varkappa+(\mu+r\varsigma)\rho}}{1 - e^{\Delta T_{\min}}}.$$

Case 2: $t \in [s_k, t_{k+1})$**.** During the resting interval,

$$\Psi(t) \leq \tilde{\Psi}(t_k^+)e^{-r(s_k-\varsigma-t_k)+(a_2+a_3)(t-s_k)}.$$

Substituting the iterative estimate of $\tilde{\Psi}(t_k^+)$, including the partial resting interval $[s_k, t)$ in the accumulated resting duration, and using the same geometricseries estimate as in Case 1 yields

$$\Psi(t) \leq \tilde{\Psi}(t_0^+)e^{\Delta(t-t_0)+(r+a_2+a_3)\varkappa+(\mu+r\varsigma)\rho} + \frac{me^{(r+a_2+a_3)\varkappa+(\mu+r\varsigma)\rho}}{1-e^{\Delta T_{\min}}}.$$

Therefore, the above estimate holds for every $t \in [t_k, t_{k+1})$. Because $\Delta < 0$,

$$\lim_{t\to\infty} \tilde{\Psi}(t_0^+)e^{\Delta(t-t_0)+(r+a_2+a_3)\varkappa+(\mu+r\varsigma)\rho} = 0.$$

Combining the above two cases, we conclude that, for any t,

$$\limsup_{t\to\infty} \Psi(t) \leq \frac{me^{(r+a_2+a_3)\varkappa+(\mu+r\varsigma)\rho}}{1-e^{\Delta T_{\min}}}.$$

This concludes the proof.

AIMS Press